Total-energy calculations for acetylene adsorption and decomposition on Si(100)-2×1

Ru-Hong Zhou, Pei-Lin Cao, and Lie-Quan Lee

*China Center of Advanced Science and Technology (World Laboratory), P.O. Box 8730, Beijing 100080, People's Republic of China
and Department of Physics, Zhejiang University, Hangzhou 310027, People's Republic of China**

(Received 13 July 1992)

The adsorbed states and vibrational properties of acetylene on Si(100)-2×1 have been studied using a molecular cluster model and the atom-superposition and electron-delocalization molecular-orbital theory. Acetylene is determined to di-σ bond to the surface dimer sites. Its C—C bond order decreases to between single and double, while its C—H bonds are only slightly weakened. The bonding angles HCC, HCSi, and SiCC of adsorbed $C_2H_2(a)$ are close to ethylenic values. Both the acetylene π donation to the surface and substrate backdonation to the acetylene π^* orbital result from the equilibrium di-σ bonding geometry. The decomposition paths and activation barriers of $C_2H_2(a)$ on Si(100) have been analyzed in detail. The calculated vibrational properties of $C_2H_2(a)$ and C_2H_2-induced species confirm the results of a recent high-resolution electron-energy-loss study.

I. INTRODUCTION

The interaction of unsaturated hydrocarbons with transition-metal surfaces has been the object of numerous studies as a prototype for the interaction of olefin hydrocarbons with catalysts.[1-8] However, the reaction of hydrocarbons with well-defined semiconductor surfaces, e.g., Si(100) and Si(111), is comparatively less studied and relatively little is known about the adsorption process and interaction mechanism. On the other hand, the adsorption of C_2H_2, C_2H_4, etc. on the Si surfaces is also of technological importance since the production of SiC thin films may be achieved by thermal decomposition of these adsorbed species. The interest in acetylene and ethylene adsorption on Si(100) (Refs. 9–11) and Si(111) (Refs. 10 and 12–14) is growing, as are the number of experimental techniques, such as high-resolution electron-energy-loss spectroscopy (HREELS),[9,10] kinetic-uptake method,[11] isotopic-mixing studies,[12] and semiempirical quantum methods.[13,14]

These recent studies have proposed a di-σ bonding geometry for $C_2H_2(C_2H_4)$ adsorption on Si(100)-2×1 (Refs. 9 and 11) with a coverage of one $C_2H_2(C_2H_4)$ molecule per Si dimer site.[11] However, no information about the bond lengths or bond angles or the decomposition paths and activation barriers has been presented. To shed some light on this problem, a theoretical calculation for the total-energy surface may be very valuable. Considering that *ab initio* methods are difficult to use with systems containing many electrons, we employ a simple molecular-orbital theory to assist our understanding and with only modes demands on computer resources.

II. MODELS AND METHOD

In this paper, a four-layer silicon-cluster model $Si_{29}H_{24}$-C_2H_2 is adopted to simulate the C_2H_2 adsorption and decomposition on Si(100)-2×1 (see Fig. 1). For this reconstructed surface, we use the (2×1) symmetric dimer model reported by Roberts and Needs.[15] According

to this model, the displacements of the first-layer Si atoms making up each dimer are 0.331 Å in the [$\bar{1}$00] direction (closer to the second layer) and ±0.803 Å in the [0$\bar{1}$1] direction (to form dimers). The second, third, and fourth layers of Si atoms also have small displacements with respect to their unreconstructed bulk places. The H atoms in the cluster model are only used to saturate the bulk Si dangling bonds as treated in most previous studies.
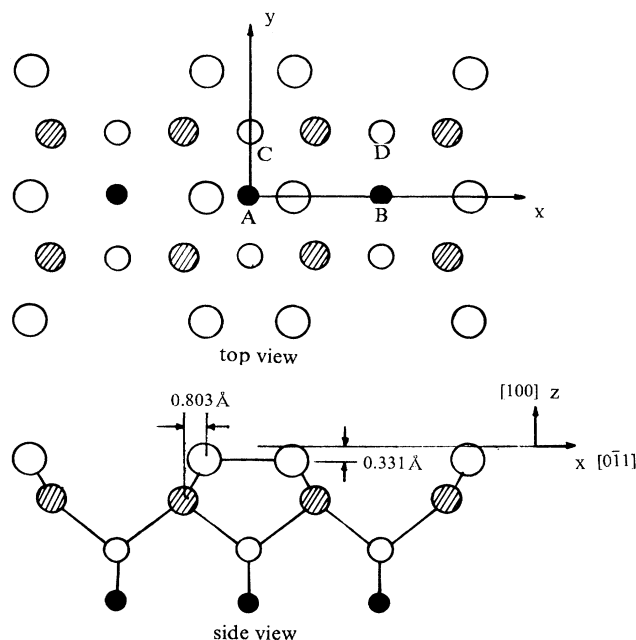

FIG. 1. Cluster model $Si_{29}H_{24}$ applied to simulate the Si(100)-2×1 surface. H atoms are used to saturate the bulk dangling bonds and are not plotted for convenience. (a) top view; (b) side view. Large open circle: first-layer Si atom; hatched circle: second-layer Si atom; small open circle: third-layer Si atom; filled circle: fourth-layer Si atom.

TABLE I. Atomic parameters used in calculations: principal quantum number (n), ionization potential [IP (eV)] and Slater-orbital exponent $[\zeta \text{ (a.u.)}]$.

Atom		S			P	
	n	IP	ξ	n	IP	ξ
Si	3	14.76	1.6344	3	9.45	1.4284
C	2	15.29	1.658	2	9.96	1.618
H	1	12.30	1.20			

The atom-superposition and electron-delocalization molecular-orbital (ASEDMO) theory is used in our total-energy (TE) calculation, which has been applied to many systems.[16-19] The extended Huckel independent energy represents the binding part of the interaction energy, which is due to electron delocalization, while the atom-superposition energy is the sum of repulsive interatomic interactions. This fast method seems appropriate especially for calculating bond geometries and force constants of complex systems. The atomic parameters used in calculations are listed in Table I. They are based on ionization potentials[20] in the literature and Slater-orbital exponents[21] with 1.3-eV shifts in the ionization potentials that produce reasonable diatomic SiC charge transfers (increases for Si and decreases for C and H). Using these parameters, the $C\equiv C$ and $C-H$ bond lengths of the free C_2H_2 molecule are overestimated by 0.11 and 0.09 Å, while the CH-stretch, CC-stretch, and CH-bend frequencies are 3299, 1945, and 718 cm^{-1}, respectively, in good agreement with the experimental results 3374, 1974, and 729 cm^{-1} (Ref. 22) (relative errors are only 2.22%, 1.47%, and 1.51%, respectively).

III. RESULTS AND DISCUSSION

A. Acetylene adsorption

As a first step, we studied the chemisorption of molecular acetylene. Four possible adsorption sites are considered in our calculations, including bridge A, cave B, pedestal C, and valley bridge D, as shown in Fig. 1. For each adsorption site, we calculated the TE curve versus the adsorption height. Here, the adsorption height (h) is defined as the vertical distance of the $C\equiv C$ triple bond from the unreconstructed Si(100) surface. That is, the height from the actual surface Si atoms is $(h +0.331 \text{ Å})$ according to the (2×1) symmetric dimer model.[15] The TE at infinite adsorption height is set to zero. For convenience, we started with two simple cases: one is the linear C_2H_2 adsorption (just free molecules) and the other is the distorted C_2H_2 adsorption with the HCC angle set at 120° (such as ethylenic species, represented by $C_2H_2^*$ in the following). Figures 2(a)-2(d) show the TE curves for the two different structures on bridge, cave, pedestal, and valley bridge sites, respectively. It is obvious that the linear C_2H_2 is energetically unfavorable, while the distorted $C_2H_2^*$ can adsorb onto the bridge site (the dimer site) to form a di-σ bonding geometry. However, this distorted $C_2H_2^*$ structure cannot adsorb onto the pedestal

and valley bridge sites [see Fig. 2(c) and 2(d)] because the TE curves increase monotonically as the $C_2H_2^*$ nears the surface. For the cave site, although a minimum appears in the TE curve [Fig. 2(b)], this energy is still much higher than zero, so $C_2H_2^*$ may also not adsorb onto the cave site.

The above two special cases demonstrate useful and direct information about the acetylene bonding on Si(100), but they are simple and incomplete. In order to have a better understanding of the bonding structure, we calculated the TE curves versus the $C\equiv C$ and $C-H$ bond lengths and HCC distorted angle. Detailed calculations show that the acetylene bonding on the cave, pedestal, and valley bridge sites are impossible. This is because of the poor overlap of C_2H_2 orbitals with surface dangling bonds on these sites.

The only possible site is the bridge site, i.e., the dimer site. Figures 3(a) and 3(b) show the variation of TE with $C-C$ bond length dc-c and HCC angle θ, respectively. The final equilibrium di-σ bonding geometry is shown in Fig. 4. The $C-C$ bond length stretches 0.18 Å to a value between double and single bond, indicating a drastic weakening of the $C\equiv C$ triple bond (later vibrational frequency calculations also confirm this). The distorted HCC angle is 123°, close to the ethylenic value. The Si—C bond length is determined to be 1.98 Å, a little larger than the bond length of β-SiC crystal 1.89 Å (Ref. 23) (the sum of the two covalent radii is 1.88 Å). The angle SiCC is only 101°, somewhat smaller than the ethylenic value. This angle may be underestimated due to the overestimate of the $C-C$ bond length for free (1.31 Å) and adsorbed C_2H_2 (1.49 Å), and the small Si-Si distance 2.23 Å for this dimer model[15] [former accepted Si—Si dimer length is ~ 2.5 Å (Ref. 24)]. HREELS spectra[9] have shown that the symmetric Si—C stretching vibration (690 cm^{-1}) is excited predominantly by the dipole mechanism. Considering the surface-normal dipole selection rule for dipole scattering, a nearly normal direction for the Si—C bond axes has been suggested.[9] Fortunately, our smaller SiCC angle [Si—C bond axes are tilted 11° with respect to the Si(100) surface normal] is more appropriate for the experimental phenomena. On the other hand, the C—H bond length stretches only 0.02 Å, and vibrational frequency calculations show a small decrease (only $\sim 11\%$) in CH frequency, which indicates the C—H bond is only slightly weakened. This is consistent with the very recent result obtained by Weiner, Carmer, and Frenklach in their calculations for C_2H_2 on Si(111) using the Zerner intermediate-neglect-of-differential-overlap semiempirical theory.[14]

Why does acetylene favor distortion on the Si(100) surface? As we know, the free molecule unequivocally favors the linear structure (ASED theory has shown the free C_2H_2 distortion costs ~ 2.9 eV, see Fig. 2). A reasonable explanation may be obtained by analyzing the energy levels of free and distorted C_2H_2, and their splitting when adsorbed onto the Si(100) surface. Figure 5 shows the ground-state energy levels of free C_2H_2, distorted $C_2H_2^*$, substrate $Si_{29}H_{24}$, and adsorbed systems C_2H_2/Si, $C_2H_2^*/Si$. Here, the energy levels of C_2H_2/Si and $C_2H_2^*/Si$ are obtained from acetylene on bridge site.

It is clear that for the linear C_2H_2 adsorption, acetylene only has π_z donations to the surface because the antibonding π^* orbitals are high above the Si surface orbitals. It is difficult for substrate dangling bonds to backdonate electrons to the empty π_z^* orbital. The resulting acetylene charge is $+0.30e$, consistent with the π_z donation model. Despite the stability obtained by this π_z donation, it is not strong enough to cancel the repulsive interaction acted on C and H atoms from substrate. This is why the linear C_2H_2 cannot adsorb onto the Si(100) surface. However, the situation for distorted $C_2H_2^*$ adsorption is very different. The distortion causes π and π^* orbitals to split into two levels. In particular, the π_z^* orbital decreases ~ 2.6 eV to a position where it can be strongly backdonated by the Si surface radicals. Meanwhile, the π_z donations are also enhanced. So, for the $C_2H_2^*$ adsorption, both the π_z donation and π_z^* backdonation occur, which result in the equilibrium ethylenic structure with a binding energy of 1.24 eV. The resulting C_2H_2 charge of $-0.21e$ also confirms this donation and backdonation model.

In order to provide further confirmation for the di-σ bonding geometry, we calculated the vibrational frequencies of C—C, C—H, Si—C, etc. bonds to compare with the recent HREELS study. We use a Morse-type expression to simulate the TE curve versus the adsorption height or bond length near the equilibrium positions:[25]

$$E(x) = E_0 + [a + b(x - x_0)$$
$$+ c(x - x_0)^2][1 - e^{-\alpha(x - x_0)}]^2 ,$$

where $E(x)$ is the TE at position x, x is the adsorption height or bond length, x_0, E_0, a, b, c, and α are the parameters to find. Using this expression, we can obtain the equilibrium position x_0, minimum TE E_0, and force constants $k = (d^2E)/(dx^2)|_{x = x_0} = 2a\alpha^2$. A series of calculations have shown that this Morse-type expression can give a more accurate force constant than the usual simple treatment using $E(x) = E_0 + b(x - x_0) + c(x - x_0)^2$. A detailed analysis of this vibrational frequency calculation method is summarized in another paper.[26]
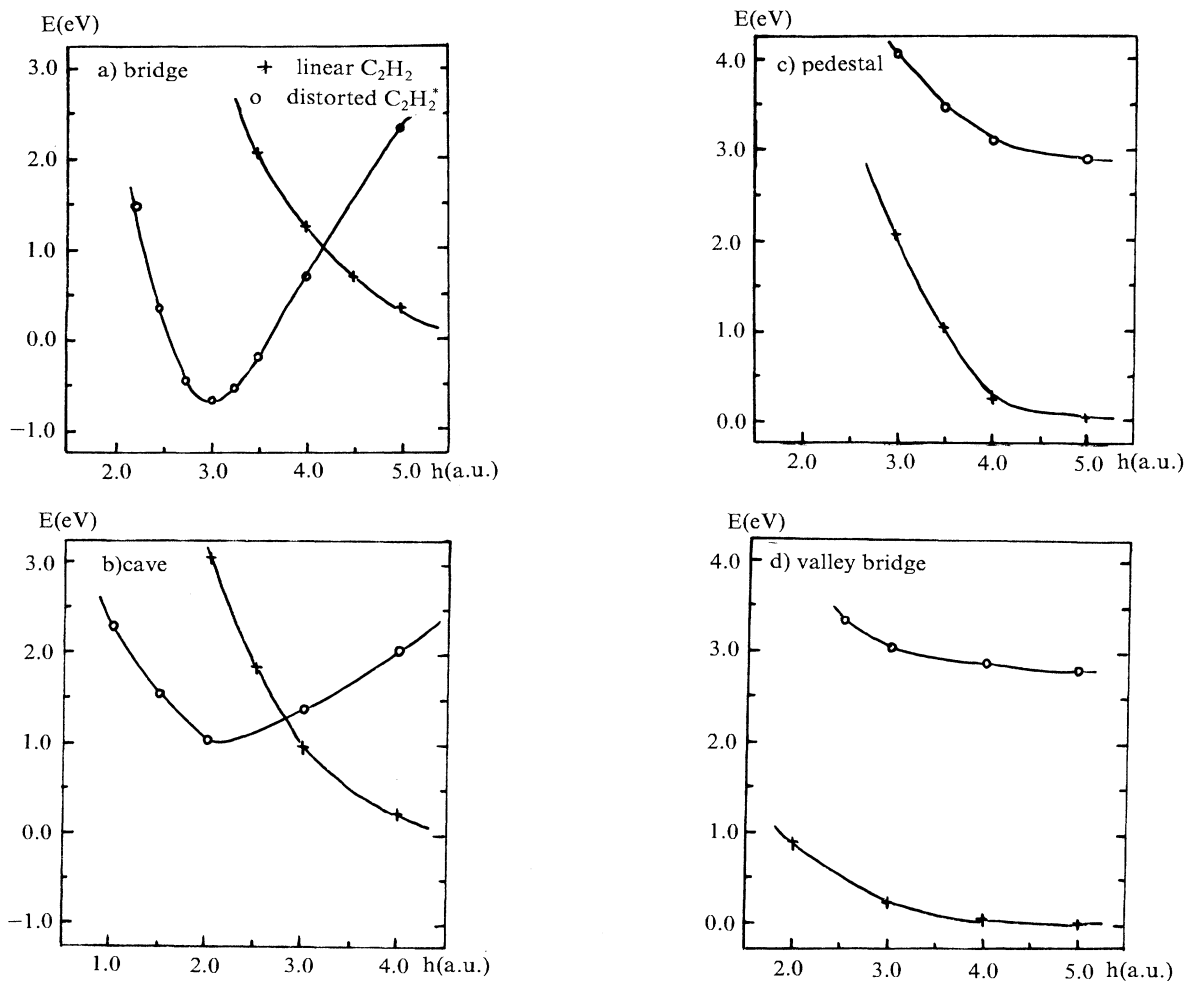

FIG. 2. Total-energy E curves vs the adsorption height h for the linear C_2H_2 (denoted by $+$) and distorted $C_2H_2^*$ (denoted by O) adsorption cases on the four adsorption sites. (a) bridge; (b) cave; (c) pedestal; (d) valley bridge.
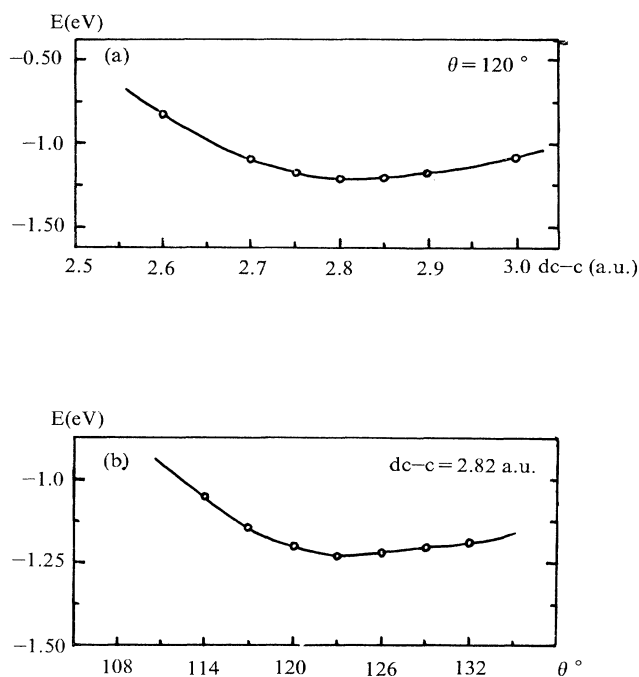
FIG. 3. Total-energy E curves vs (a) the C—C bond length dc-c and (b) the HCC bond angle θ for C_2H_2 adsorbed on the dimer site (i.e., bridge).

TABLE II. Calculated vibrational energies of C_2H_2 and C_2H_2-induced species on Si(100)-2×1. The vibrational energies for free gas (Ref. 22) and recent HREELS results (Ref. 9) are included for comparison.

Mode	Free C_2H_2 Theor.	Expt.	Adsorbed C_2H_2 Theor.	Expt.
CH stretch	3329	3374	2958	3000
CC stretch	1945	1974	978–1383	1090
CH bend	718	729	1047	970–1255
SiC stretch (C_2H_2)			653	690
SiH stretch			2124	~2120
SiC stretch			773	800

ists between C—C stretching and Si—C stretching, i.e., the reduced mass is ~ 13.0 a.u., while, on the other hand, if we propose that there is only a weak coupling between C—C and Si—C stretching, i.e., the reduced mass is $\sim \frac{13}{2}$ a.u., the C—C stretching energy will be 1383 cm^{-1}. The experimental C—C stretching value 1090 cm^{-1} falls in the range 978–1383 cm^{-1}. Overall, our calculated vibrational frequencies are consistent with the experimental values, which confirm the suggestion of the HREELS study for the bonding geometry.

The frequencies of decomposed C and H atoms on

Table II lists the calculated and observed vibrational frequencies for free gas and adsorbed C_2H_2 on dimer site. As mentioned in Sec. I, the relative errors of theoretical and experimental frequencies for free C_2H_2 are very small. For the adsorbed C_2H_2, the CH stretching energy decreases from 3329 to 2958 cm^{-1} (decrease $\sim 11\%$), in good agreement with the HREELS result form 3374 to 3000 cm^{-1} (also decrease $\sim 11\%$).[9] The CH bending energy is determined to be 1047 cm^{-1}, which is in the range of observed symmetric and asymmetric values 970–1255 cm^{-1}. The force constants of C—C stretching is predicted to be 12.95 eV/a.u.[2] The C—C stretching energy will be 978 cm^{-1} if we propose that a very strong coupling ex-
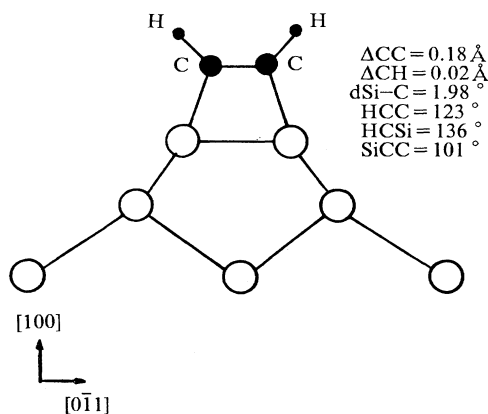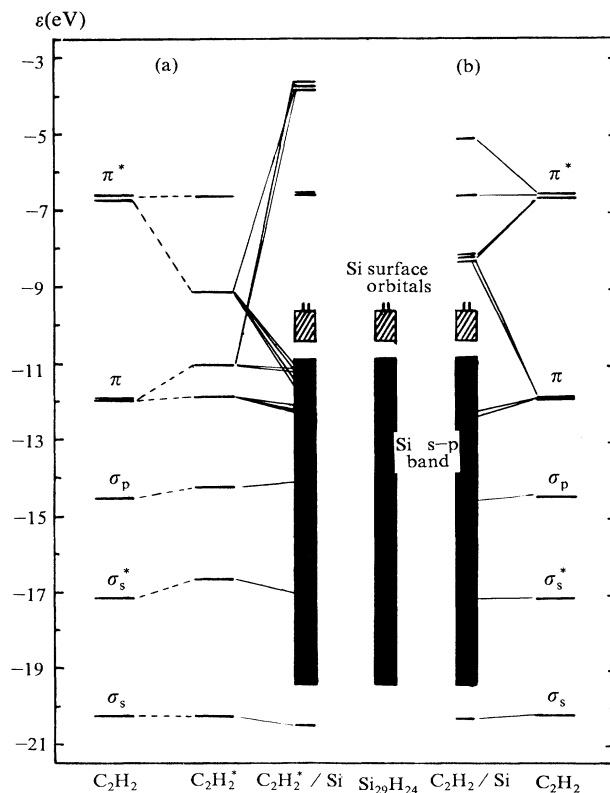

$\Delta CC = 0.18$ Å
$\Delta CH = 0.02$ Å
dSi—$C = 1.98$ °
$HCC = 123$ °
$HCSi = 136$ °
$SiCC = 101$ °

[100]

[0$\bar{1}$1]

FIG. 4. Adsorption geometry for the di-σ bonded C_2H_2 on dimer sites.

FIG. 5. Ground-state energy levels of free C_2H_2, distorted $C_2H_2^*$, substrate $Si_{29}H_{24}$, and adsorbed systems C_2H_2/Si, $C_2H_2^*/Si$ for C_2H_2 adsorption on the dimer site.

Si(100) are also included in Table II (the bonding structures will be discussed later). They are in excellent agreement with the experimental values, which confirms again the validity of the simple method for vibrational frequency calculation.

B. Decomposition of C_2H_2

Since the decomposition of C_2H_4, C_2H_2, etc. small molecules on Si(100) can make it possible for the growth of high-quality single-crystal β-SiC films,[11,12,14] we studied the dissociation process of C_2H_2 on Si(100). A favored decomposition path $C_2H_2 \rightarrow C_2H_x$ $(x = 0,1) \rightarrow C \rightarrow \beta$-SiC is proposed.

At first, we calculated the dissociation path for one H atom from the adsorbed C_2H_2. Figures 6 and 7 show the H dissociation paths in xz and yz planes (the coordinates are shown in Fig. 1). The path steps of 0.2 a.u. are adopted for H-atom migration in x, y, and z directions. For each x (or y) value, we can obtain the optimized z value from the TE minimum. Thus, an optimum dissociation path and the resulting TE variation curve can be obtained (see Figs. 6 and 7). We found an activation barrier of 1.07 and 0.94 eV in xz and yz planes, respectively. In fact, the H atom may dissociate in any directions on Si(100) surface, but we can estimate the actual activation barrier by analyzing these two special cases. Further considering the optimization of the residual part CCH

(ethynyl), we predict the activation barrier to be no less than 0.8 eV, which is comparable to the C_2H_2 binding energy 1.24 eV. This is why C_2H_2 is predominantly chemisorbed nondissociatively between 80 and ~ 300 K.[9] And it also explains the phenomenon that when heating to 750 K, some of the chemisorbed C_2H_2 is desorbed while some is decomposed to C_2H_x $(x = 0,1)$ and H species.[9]

The dissociation of the remaining C_2 species is calculated to have a barrier of 1.30 eV. While the decomposition of C_2H_2 directly to C_1H_1 (methylidyne) species is determined to be endothermic by ~ 2.2 eV. This indicates that acetylene favors dehydrogenation to C_2H_x $(x = 0,1)$ species first; then the remaining C_2 further decompose to C species to form β-SiC films, rather than to form C_1H_1 species directly.

This is somewhat different from the cases for C_2H_2 decomposition on transition metals. On Pd(100), C_2H_2 is dehydrogenated to form CCH at 450 K.[1] Acetylene chemisorbed on Pd(111) (Ref. 1) and Ru(0001) (Ref. 2) is dehydrogenated to form both CCH and CCH_3 (ethylidyne) at ~ 300 and 230 K, respectively. On Pt(111), CCH_2 (vinylidene) has been proposed as the intermediate in C_2H_2 dehydrogenation.[3] On Ni(111) (Ref. 4) and Fe(110) (Ref. 5), C_2H_2 is dehydrogenated to CH at 400 and 340 K, respectively, while on Mo(100),[7] C_2H_2 is dehydrogenated to CCH at as low as 180 K, and our ASED study for this dissociation path revealed no significant activation barriers. Similarly, Kang and Anderson, using ASED theory, found almost no barrier in
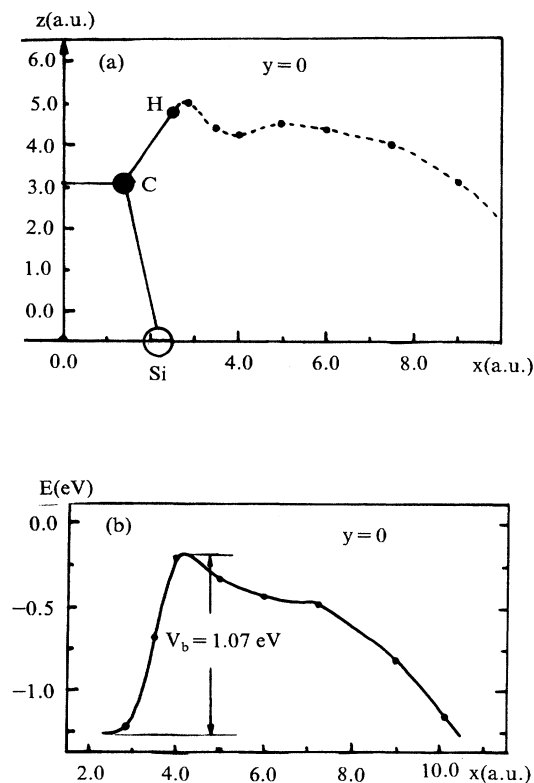

FIG. 6. (a) Optimized dissociation path for H atom in the xz plane. (b) The corresponding total-energy E variation curve showing an activation barrier of 1.07 eV.
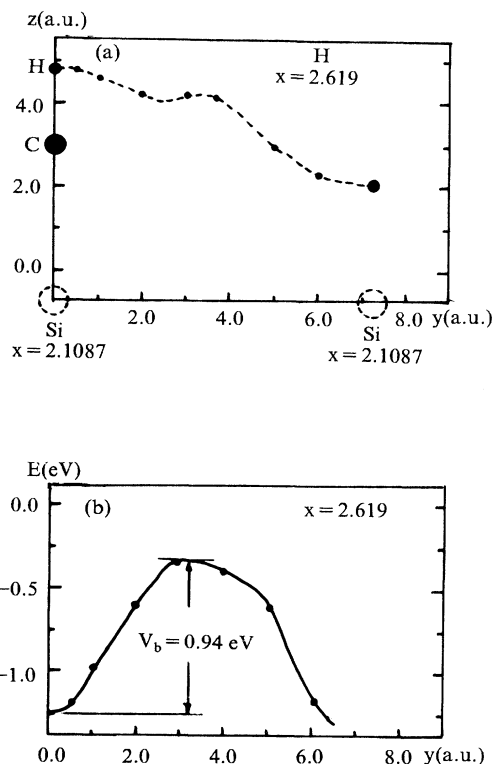

FIG. 7. Same as in Fig. 6 but for H-atom dissociation in the yz plane, showing a barrier of 0.94 eV.

the dissociation process of $C_2H_2 \rightarrow CCH$ on Pt(111), and only a 0.4-eV barrier in the further decomposition of $CCH \rightarrow CH + C$. In summary, acetylene on transition metals will produce many more intermediates than that on Si surfaces, and in most cases the decomposition on transition metals is much easier than that on Si surfaces.

Finally, the bonding geometries of dissociated C and H atoms are discussed. Both C and H atoms adsorb onto the surface dangling bonds. The Si—C bond length is optimized to be 1.75 Å, 0.23 Å less than that for the adsorbed C_2H_2 molecule (1.98 Å), and is very close to the diatomic Si—C bond length of 1.70 Å.[27] The angle of the Si—C bond to the surface normal is close to 19°, and the binding energy is 2.17 eV. The Si—H bond is very similar to the Si—C bond, but with a bond length of 1.56 Å and binding energy of 1.65 eV. The Si—C and Si—H stretching frequencies are calculated to be 773 and 2124 cm^{-1}, respectively, in excellent agreement with the observed 800 and $\sim$2120 cm^{-1}.[9]

IV. CONCLUSIONS

The adsorption and decomposition of acetylene on the Si(100)-2×1 surface, as well as the vibrational properties, have been studied by total-energy surface calculations. A summary of the important results are collected as follows.

(i) Acetylene is di-σ bonded to the surface dimer sites with C—C and C—H bond lengths stretching 0.18 and 0.02 Å, respectively. The Si—C bond length is 1.98 Å, and the bond angles HCC, HCSi, and SiCC are close to ethylenic values.

(ii) The $C \equiv C$ triple bond is transformed to a bond between single and double, while the C—H bond is only slightly weakened.

(iii) In the adsorption process, the linear C_2H_2 only has π donations to the surface, while the distorted $C_2H_2^*$ has both π donations and π^* backdonations from surface radicals, which result in the equilibrium di-σ bonding geometry (distorted).

(iv) The decomposition of C_2H_2 on Si(100) is somewhat different from that on transition metals. Acetylene favors a decomposition path of $C_2H_2 \rightarrow C_2H_x$ $(x = 0, 1) \rightarrow C_2 \rightarrow C$ rather than $C_2H_2 \rightarrow CH \rightarrow C + H$. The activation barrier for H dissociation from C_2H_2 is estimated to be 0.8 eV. The further decomposition of $C_2 \rightarrow C$ is found to be endothermic by 1.3 eV.

(v) The vibrational properties are calculated in detail. All the results are in good agreement with the observed values, which confirms the suggestion of di-σ bonding geometry by HREELS spectra.

*Address to which correspondence should be sent.

[1] L. L. Kesmodel, G. D. Waddill, and J. A. Gates, Surf. Sci. **138**, 464 (1984).

[2] J. E. Parmeter M. M. Hills, and W. H. Weinberg, J. Am. Chem. Soc. **108**, 3563 (1986).

[3] H. Ibach and S. Lekwald, J. Vac. Sci. Technol. **15**, 407 (1978).

[4] S. Lehwald and H. Ibach, Surf. Sci. **89**, 425 (1979).

[5] W. Erley, A. M. Baro, and H. Ibach, Surf. Sci. **120**, 273 (1982).

[6] W. Erley, N. J. Dinardo, J. E. Demuth, and P. Avouris, Phys. Rev. B **27**, 5832 (1983).

[7] L. Wang and W. Tysoe, Surf. Sci. **230**, 74 (1990).

[8] D. B. Kang and A. B. Anderson, Surf. Sci. **155**, 639 (1985).

[9] M. Nishijima, J. Yoshinobu, H. Tsuda, and M. Onchi, Surf. Sci. **192**, 383 (1987).

[10] J. Yoshinubu, H. Tsuda, M. Onchi, and M. Nishijima, Chem. Phys. Lett. **30**, 170 (1986); Solid State Commun. **60**, 801 (1986); J. Chem. Phys. **87**, 733 (1987).

[11] C. C. Cheng, R. M. Wallace, P. A. Taylor, W. J. Choyke, and J. T. Yates, Jr., J. Appl. Phys. **67**, 3693 (1990).

[12] C. C. Cheng, W. J. Choyke, and J. T. Yates, Jr., Surf. Sci. **231**, 289 (1990).

[13] S. Y. Chu and A. B. Anderson, Surf. Sci. **194**, 55 (1988).

[14] B. Weiner, C. S. Carmer, and M. Frenklach, Phys. Rev. B **43**, 1678 (1991).

[15] N. Roberts and R. J. Needs, Surf. Sci. **236**, 112 (1990).

[16] D. Domanek and K. H. Bennemann, Phys. Rev. B **31**, 2485 (1985).

[17] Pei-Lin Cao and Zhong-Guo Zhang, Phys. Rev. B **39**, 9963 (1989).

[18] Ru-Hong Zhou, Dai-Hua Shi, and Pei-Lin Cao, J. Phys. Condens. Matter **4**, 2429 (1992).

[19] Pei-Lin Cao, Ru-Hong Zhou, and Xu-Yan Zhou, Phys. Lett. A **159**, 179 (1991).

[20] W. Lotz, J. Opt. Soc. Am. **60**, 206 (1970).

[21] E. Clementi and D. L. Raimondi, J. Chem. Phys. **38**, 2686 (1963).

[22] G. Hertzberg, *Infrared and Raman Spectra of Polyatomic Molecules*, Molecular Spectra and Molecular Structure Vol. II (Van Nostrand, New York, 1945).

[23] J. D. H. Donnay and H. M. Ondik, *Inorganic Compounds, Crystal Data, Determinative Tables*, 3rd ed. Vol. II (U.S. GPO, Washington, DC, 1973).

[24] D. J. Chadi, Phys. Rev. Lett. **43**, 43 (1979).

[25] Ru-Hong Zhou and Pei-Lin Cao, Surf. Sci. (to be published).

[26] Ru-Hong Zhou and Pei-Lin Cao (unpublished).

[27] Molecular Spectra and Molecular Structure Vol. VI, Constants of Diatomic Molecule, edited by K. P. Huber and G. Hertzberg (Van Nostrand, New York, 1979),Vol. VI.